Original Article

Development and validation of a screening model for benign and malignant breast masses based on S-Detect and microvascular flow imaging

Zhongguang Hou, Yunyun Zhan, Jiajia Wang, Mei Peng

Department of Ultrasound, Second Affiliated Hospital of Anhui Medical University, Hefei, China

Contributions: (I) Conception and design: Z Hou, J Wang, M Peng; (II) Administrative support: M Peng; (III) Provision of study materials or patients: Y Zhan, J Wang, M Peng; (IV) Collection and assembly of data: Z Hou, Y Zhan; (V) Data analysis and interpretation: Z Hou; (VI) Manuscript writing: All authors; (VII) Final approval of manuscript: All authors.

Correspondence to: Mei Peng, Master's Degree; Jiajia Wang, MD, PhD. Department of Ultrasound, Second Affiliated Hospital of Anhui Medical University, No. 678, Furong Road, Economic and Technological Development Zone, Hefei 230000, China. Email: 13955125956@163.com; ahmuwangjiajia@163.com.

Background: Imaging examination of a breast mass is essential for improving breast cancer detection. Previous screening models of benign and malignant breast masses demonstrated a high level of subjectivity due to the inability to conduct quantitative evaluations. Thus, this study aimed to construct an objective, convenient, and effective nomogram incorporating S-Detect and microvascular flow imaging (MVFI) to predict breast cancer risk.

Methods: Female patients with breast masses detected by conventional ultrasound examinations at the Second Affiliated Hospital of Anhui Medical University between January 2021 and October 2024 were retrospectively analyzed. All patients underwent preoperative assessments with both S-Detect and MVFI. The pathological results served as the gold standard for diagnosis. After screening, a total of 724 breast masses from 712 patients were randomized into the training (506 masses) and validation (218 masses) groups. Univariate analysis assessed patient age, as well as the location, size, vascular index (VI), and S-Detect-based diagnosis of the masses. Risk factors for predicting breast cancer were screened using multivariate analysis. A nomogram prediction model was then constructed. Diagnostic performance, clinical utilization value, and calibration were determined using the receiver operating characteristic (ROC) curve, decision curve analysis (DCA), and calibration curve, respectively. Nomogram risk was calculated for each breast mass for risk stratification.

Results: The training group included 208 benign and 298 malignant masses, while the validation group comprised 85 benign and 133 malignant masses. Multivariate analysis demonstrated that mass size [odds ratio (OR) =1.08; P<0.001], age (OR =1.09; P<0.001), VI (OR =1.07; P<0.001), and S-Detect-based diagnosis (OR =28.37; P<0.001) were risk factors for predicting breast cancer. The area under the curve (AUC) for the nomogram model was significantly greater than that for S-Detect in both the training (0.93 *vs.* 0.82, P<0.001) and validation (0.91 *vs.* 0.82, P<0.001) groups. The diagnostic sensitivity and specificity of the nomogram were 93.3% and 79.8% in the training group, and 98.5% and 72.9% in the validation group, respectively. The optimal cut-off value for nomogram risk differentiation between the high-risk and low-risk sets was 0.495, with a significantly higher proportion of malignant breast masses in the high-risk set compared to that in the low-risk set (P<0.001).

Conclusions: This novel nomogram model based on quantitative and objective ultrasound and clinical features can quantify the malignancy risk of breast masses, identify high-risk individuals, and provide a reference for further examinations.

Keywords: Breast cancer; ultrasound; S-Detect; nomogram

Submitted Nov 08, 2024. Accepted for publication Mar 24, 2025. Published online Apr 22, 2025.
doi: 10.21037/gs-2024-488
View this article at: https://dx.doi.org/10.21037/gs-2024-488

Introduction

Breast cancer is the most prevalent type of cancer worldwide in women (1,2). The incidence rates of breast cancer in young women are increasing annually in numerous countries (3). The type of breast cancer affecting young women is often more aggressive compared to that in older women and warrants increased attention (4). The implementation of breast cancer screening improves the rate of early diagnosis, which is a crucial first step in improving the prognosis of patients and reducing mortality (5). In high-income countries, mammography-based screening is considered the most common method for detecting breast cancer (6). Over the past few decades, mammography-based screening has been effective in decreasing breast cancer-associated deaths and improving patient prognosis, contributing to a >20% reduction in breast cancer mortality in women aged 50–69 years (7). Mammography exhibits a sensitivity of approximately 85% for the identification of breast cancer. However, it is not ideal for women with dense breast tissue, and it is sometimes difficult to differentiate between diseased and normal tissue with a sensitivity of only 47.8–64.4% (8). Chinese women have a higher percentage of dense breasts, and mammography-based screening has significant limitations in this population. A previous multi-center study demonstrated that ultrasound can be an effective tool for screening breast cancer in women with dense breasts, exhibiting superior sensitivity and specificity, and with a lower cost than mammography (9). In China, ultrasound is extensively used for breast cancer screening due to its simplicity, lack of radiation exposure, and real-time dynamics.

Currently, the Breast Imaging Reporting and Data System (BI-RADS) serves as a crucial foundation for the standardized assessment of breast mass risk (10). However, ultrasound also has limitations and requires examination with a handheld device by an experienced sonologist. The assessment of breast masses is affected by subjective factors such as the skill, experience, and diagnostic ability of the sonologists, and some atypical breast masses can be easily misdiagnosed, especially in some primary healthcare services (11). Moreover, the process of breast cancer screening is intensive and repetitive, which may lead to errors due to personnel fatigue. Several prediction models have been developed based on the ultrasound features available for distinguishing between benign and malignant breast masses. He *et al.* (12) constructed a prediction model of benign and malignant breast masses, which included the patient's clinical features and BI-RADS-based ultrasound characteristics as the model predictors. This prediction model achieved an area under the curve (AUC) of 0.952. However, the model encompasses 12 predictors, which increase the workload involved in the breast cancer screening process. Furthermore, the ultrasound features, including irregular shape, irregular border, heterogeneous echo, microcalcification, and attenuation effects, are heavily dependent on the subjective assessment of experienced sonologists. In the model constructed by Yan *et al.* (13), predictors incorporated both conventional ultrasound and contrast-enhanced ultrasound features. This model demonstrated high diagnostic performance, achieving an AUC of 0.940. However, it is limited by longer exam

Highlight box

Key findings

- We developed a breast cancer prediction model based on quantitative and objective clinical and ultrasound characteristics to aid in screening of breast cancer.

What is known and what is new?

- Ultrasound is extensively used for breast cancer screening due to its simplicity, lack of radiation exposure, and real-time dynamics. However, it is affected by subjective factors such as the sonologists' skill, experience, and diagnostic ability.
- S-Detect can automatically extract and analyze the ultrasound image characteristics based on the Breast Imaging Reporting and Data System lexicon and objectively provide diagnoses of "possibly benign" and "possibly malignant" breast masses. Microvascular flow imaging enables the sensitive detection of low-flow microvessels, which can be quantified using vascular index. We constructed a nomogram model based on the ultrasound characteristics.

What is the implication, and what should change now?

- The newly constructed nomogram model can quantify the malignancy risk of breast masses, providing a reliable and objective initial assessment to help screen breast cancer while minimizing the influence of subjective judgment.

durations and higher costs of contrast-enhanced ultrasound, as well as the potential risk of contrast agent allergy, making it unsuitable for mass breast cancer screening.

With the rapid development of technology, many new ultrasound methods are gradually being applied in clinical practice. Artificial intelligence (AI) has been utilized in the analysis of ultrasound images to help diagnose breast masses (14). Ultrasound S-Detect technology is based on convolutional neural networks and deep learning algorithms and is one of the most common AI technologies for evaluating breast masses (15). Ultrasound limitations can be overcome by using S-Detect, which can automatically extract and analyze ultrasound image features based on the BI-RADS lexicon, reducing the influence of subjective human factors. S-Detect can also objectively provide "possibly benign" and "possibly malignant" diagnoses. Indeed, a prospective multi-center study demonstrated that S-Detect has a high diagnostic value in distinguishing between benign and malignant breast masses, with a diagnostic AUC of 0.906, which is significantly higher than that of both experienced and less experienced sonologists (16). Although the performance of S-Detect in diagnosing breast lesions varies across studies, all of them affirm its clinical value in diagnosing breast cancer and its ability to effectively reduce the impact of subjective factors on diagnostic results, thereby improving the accuracy and reliability of the diagnosis (17). However, S-Detect technology cannot analyze the distribution of blood vessels within the mass. Breast cancer exhibits significant vascular dependency during its onset and progression, with its growth, invasion, and metastasis often accompanied by extensive angiogenesis (18). Malignant masses generally have a more complex and abundant network of blood vessels compared to benign masses (19). As a novel ultrasound technology, microvascular flow imaging (MVFI) can quickly and non-invasively visualize low-velocity microvessels within a breast mass, while the vascular index (VI) enables quantitative evaluation. Previous studies have indicated that the VI can help in distinguishing between benign and malignant breast masses (18,20). Moreover, the occurrence of breast cancer is closely related to age. To the best of our knowledge, very few prediction models are based on S-Detect and MVFI. Therefore, we try to use these ultrasound features to distinguish between benign and malignant breast masses by constructing an accurate, convenient, and efficient breast cancer prediction model. The model may help to screen breast cancer while minimizing the influence of sonologists' subjective judgment. We present this article in accordance with the TRIPOD reporting checklist (available at https://gs.amegroups.com/article/view/10.21037/gs-2024-488/rc).

Methods

Sample size

In the previous study (13), predictive model achieved an AUC of 0.94. Using PASS 21.0 software for sample size estimation, a significance level of 0.05 and a margin of error of 2.5% were specified. The sample size, based on a 1:1 ratio of benign to malignant masses, is approximately 378. Thus, at least approximately 378 masses were required for this study.

Patients

The retrospective study was to described in a large patient cohort. The study received approval from the Medical Research Ethics Committee of the Second Affiliated Hospital of Anhui Medical University (No. SL-YX2022-015) and was conducted in accordance with the Declaration of Helsinki and its subsequent amendments. Individual consent was waived due to the retrospective nature of the analysis. Patients with breast masses detected by conventional ultrasound in the Second Affiliated Hospital of Anhui Medical University between January 2021 and October 2024 were identified and further screened according to the eligibility outlined below.

Inclusion criteria: (I) clear pathological findings and complete medical history after surgery or puncture biopsy; and (II) patients who underwent S-Detect and MVFI examinations before surgery. Exclusion criteria: (I) a mass >50 mm in diameter; (II) patients who had received radiotherapy before the study; and (III) patients who were pregnant or are currently breastfeeding. We evaluated 724 breast masses from 712 female patients in the final analysis. The pathology results served as the gold standard for confirming the diagnosis. *Figure 1* provides a flowchart for the screening process.

Ultrasound examinations and image analysis

All breast examinations in the study were conducted utilizing a Samsung RS85A ultrasound system (Samsung Madison Ltd., Seoul, South Korea) with a 3–12 MHz linear probe. The patients were in a supine position with both breast areas fully exposed. First, a complete sweep of

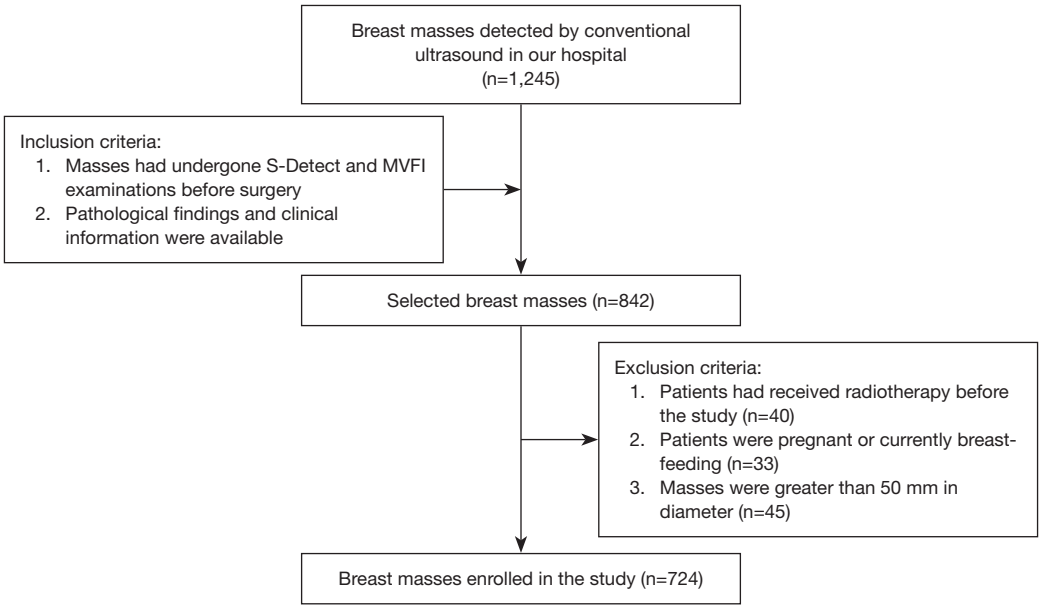

Figure 1 Screening flowchart. MVFI, microvascular flow imaging.

the breast was performed using conventional ultrasound to obtain two-dimensional grayscale images of the breast mass, recording its features (e.g., size and location). Subsequently, both of the maximum sections of the breast mass were selected and the S-Detect mode was activated. Clicking on the central area of the mass triggered the system to automatically identify and outline the mass boundary, which was manually adjusted as necessary to achieve the appropriate outline. The system then provided the diagnosis of "possibly benign" or "possibly malignant". The maximum transverse and longitudinal sections of each mass were assessed. The final diagnosis was benign when both sections of each mass were diagnosed as "possibly benign". The final diagnosis was malignant if the diagnosis in either section was "possibly malignant". Finally, MVFI was used to visualize the blood flow in the mass. The region of interest was manually delineated along the boundary of the mass in the section exhibiting the richest blood flow, with the probe gently placed on the surface to prevent the application of any pressure. The quantitative VI was calculated automatically by the software. The average of three VI measurements was recorded as the final result.

Statistical analysis

Statistical analyses were conducted using SPSS 27.0 and R 4.4.0 software. The sample size was estimated using PASS 21.0 software. Continuous variables were described as means ± standard deviation (SD) or as medians (25^{th} percentile, 75^{th} percentile), and categorical variables were represented as frequencies (percentages). Categorical variables were assessed by the Chi-squared (χ^2) test, and continuous variables were evaluated using the Mann-Whitney *U* test or Student's *t*-test. The receiver operating characteristic (ROC) curves were plotted to reflect the diagnostic performance of the nomogram and S-Detect, and the DeLong test was used to compare significant differences between the AUC. The optimal cut-off value was determined using the maximum Youden index. The sensitivity and specificity of the nomogram model at this threshold were then calculated. The nomogram model was assessed using the Hosmer-Lemeshow test, calibration curve, and decision curve analysis (DCA). P value <0.05 was considered statistically significant for a two-sided test.

Results

Clinical and ultrasound characteristics

A total of 724 breast masses were evaluated in the study. The pathology examination-based diagnosis confirmed 431 malignant and 293 benign masses. The breast masses were randomized at a 7:3 ratio into the training (506 masses; mean age: 47.81±12.96 years; range, 16–87 years) and validation (218 masses; mean age: 47.71±13.54 years;

Table 1 Breast mass characteristics

Characteristics	Total (n=724)	Training (n=506)	Validation (n=218)	Test statistics	P value
Pathology				χ^2=0.28	0.60
Benign	293 (40.47)	208 (41.11)	85 (38.99)		
Malignant	431 (59.53)	298 (58.89)	133 (61.01)		
Age (years)	47.78±13.12	47.81±12.96	47.71±13.54	*t*=−0.10	0.92
Size (mm)	22.51±9.89	22.32±9.79	22.97±10.11	*t*=0.81	0.42
VI (%)	6.30 (1.70, 12.50)	6.15 (1.40, 13.10)	6.40 (2.70, 11.95)	Z=−0.61	0.55
Location				χ^2=0.01	0.91
Left	363 (50.14)	253 (50.00)	110 (50.46)		
Right	361 (49.86)	253 (50.00)	108 (49.54)		
Quadrant distribution				χ^2=2.63	0.62
Outer upper	327 (45.17)	225 (44.47)	102 (46.79)		
Outer lower	148 (20.44)	104 (20.55)	44 (20.18)		
Inner upper	155 (21.41)	114 (22.53)	41 (18.81)		
Inner lower	67 (9.25)	47 (9.29)	20 (9.17)		
Others	27 (3.73)	16 (3.16)	11 (5.05)		
S-Detect				χ^2=1.03	0.31
Benign	232 (32.04)	168 (33.20)	64 (29.36)		
Malignant	492 (67.96)	338 (66.80)	154 (70.64)		

Data are presented as n (%), mean ± standard deviation, or median (25th percentile, 75th percentile). VI, vascular index.

range, 17–87 years) groups. The clinical and ultrasound characteristics of the breast masses are listed in *Table 1*. No significant differences were observed in any of the characteristics between the two groups (P>0.05). *Table 2* shows the univariate risk analysis of the clinical and ultrasound characteristics of the training and validation groups. There was no correlation between the location of the mass and its malignancy or benignity (P>0.05). For the ultrasound features of the mass, S-Detect-based diagnosis and VI between malignant and benign masses showed significant differences (P<0.001).

Construction of the nomogram prediction model

Characteristics that differed significantly (P<0.05) in the univariate risk analysis of the training group were incorporated into logistic regression. The results showed that age, size, VI, and S-Detect diagnosis were independent risk factors for breast cancer (P<0.05; *Table 3*). These independent risk factors were used to construct a nomogram for predicting breast cancer (*Figure 2*). The nomogram showed that the breast cancer risk for each mass can be determined by summing the points for each variable. *Figure 3* depicts an example of the practical application of the nomogram prediction model.

Assessment of the nomogram prediction model

The ROC curves were plotted to evaluate the predictive ability of the nomogram. The AUC were 0.93 [95% confidence interval (CI): 0.90–0.95] and 0.91 (95% CI: 0.86–0.96) for the training and validation groups, respectively (*Figure 4*). The nomogram AUC was higher than that of the S-Detect alone (Z=7.69, P<0.001; Z=3.829, P<0.001; respectively). The diagnostic sensitivity and specificity of the nomogram were 93.3% (95% CI: 90.4–96.1%) and 79.8% (95% CI: 74.4–85.3%) in the training group, and 98.5% (95% CI: 96.4–100.0%) and 72.9% (95% CI: 63.5–82.4%) in the validation group, respectively. The Hosmer-Lemeshow test and calibration curve demonstrated

Table 2 Univariate risk analysis of breast mass characteristics

Characteristics	Training				Validation			
	Benign (n=208)	Malignant (n=298)	Test statistics	P value	Benign (n=85)	Malignant (n=133)	Test statistics	P value
Location			χ^2=0.13	0.72			χ^2=0.10	0.76
Left	102 (49.04)	151 (50.67)			44 (51.76)	66 (49.62)		
Right	106 (50.96)	147 (49.33)			41 (48.24)	67 (50.38)		
Quadrant distribution			χ^2=2.50	0.65			χ^2=1.07	0.90
Outer upper	95 (45.67)	130 (43.62)			39 (45.88)	63 (47.37)		
Outer lower	40 (19.23)	64 (21.48)			17 (20.00)	27 (20.30)		
Inner upper	50 (24.04)	64 (21.48)			17 (20.00)	24 (18.05)		
Inner lower	19 (9.13)	28 (9.40)			9 (10.59)	11 (8.27)		
Others	4 (1.92)	12 (4.03)			3 (3.53)	8 (6.02)		
Age (years)	41.08±12.41	52.51±11.15	*t*=−10.63	<0.001	38.48±12.22	53.60±10.79	*t*=−9.32	<0.001
Size (mm)	17.84±8.74	25.44±9.27	*t*=−9.39	<0.001	20.39±10.45	24.62±9.57	*t*=−3.07	0.002
VI (%)	1.45 (0.00, 8.70)	8.45 (4.50, 15.83)	Z=−9.47	<0.001	3.00 (0.40, 8.60)	7.60 (4.80, 12.40)	Z=−4.98	<0.001
S-Detect			χ^2=229.38	<0.001			χ^2=101.54	<0.001
Benign	148 (71.15)	20 (6.71)			58 (68.24)	6 (4.51)		
Malignant	60 (28.85)	278 (93.29)			27 (31.76)	127 (95.49)		

Data are presented as n (%), mean ± standard deviation, or median (25th percentile, 75th percentile). VI, vascular index.

Table 3 Independent risk factors of breast cancer

Variables	β	P value	OR (95% CI)
Age, years	0.09	<0.001	1.09 (1.06–1.12)
Size, mm	0.08	<0.001	1.08 (1.05–1.12)
VI	0.06	<0.001	1.07 (1.04–1.10)
S-Detect	3.35	<0.001	28.37 (14.53–55.40)

CI, confidence interval; OR, odds ratio; VI, vascular index.

significant concordance between the predicted and actual results of the nomogram (χ^2=10.454, P=0.235; χ^2=12.178, P=0.143; respectively; *Figure 5*). The DCA revealed that the nomogram had a significantly higher net clinical benefit than S-Detect alone (*Figure 6*).

Risk grouping for breast masses

Total nomogram points were calculated for each breast mass, with an optimal cut-off value of 106.4 for total points and 0.495 for nomogram risk of breast masses in the training group. Breast masses with nomogram risk ≥0.495 were divided into the high-risk set, with <0.495 into the low-risk set. The proportion of malignant breast masses in the high-risk set was significantly higher than that in the low-risk set (P<0.001; *Figure 7*).

Discussion

In the study, we evaluated 724 breast masses from 712 female patients to develop a nomogram prediction model for breast cancer risk. Age, mass size, VI, and S-Detect-based diagnosis were independent risk factors for predicting breast cancer via multifactorial logistic regression analysis (P<0.05). The AUC, sensitivity, and specificity of the nomogram were 0.93, 93.3% and 79.8% in the training group and 0.91, 98.5%, and 72.9% in the validation group, respectively, demonstrating excellent prediction accuracy and sensitivity. The model showed significantly higher AUC and net clinical benefits than S-Detect. This finding indicated that the combined use of S-Detect and other indicators can effectively compensate for its limitations, thereby significantly enhancing the diagnostic accuracy for breast cancer.

A nomogram is a clinically valuable and convenient tool, offering the advantage of transforming intricate regression equations into intuitive visual graphs (21). By integrating

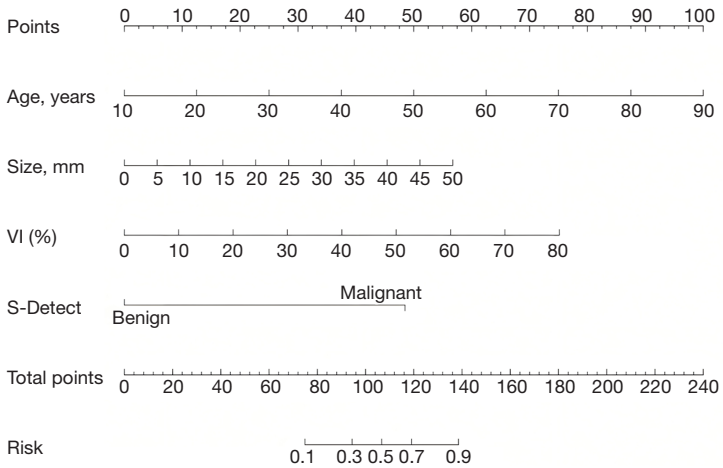

Figure 2 Nomogram prediction model for breast cancer risk. The model consists of four variable axes: age, size, VI, and S-Detect-based diagnosis. VI, vascular index.

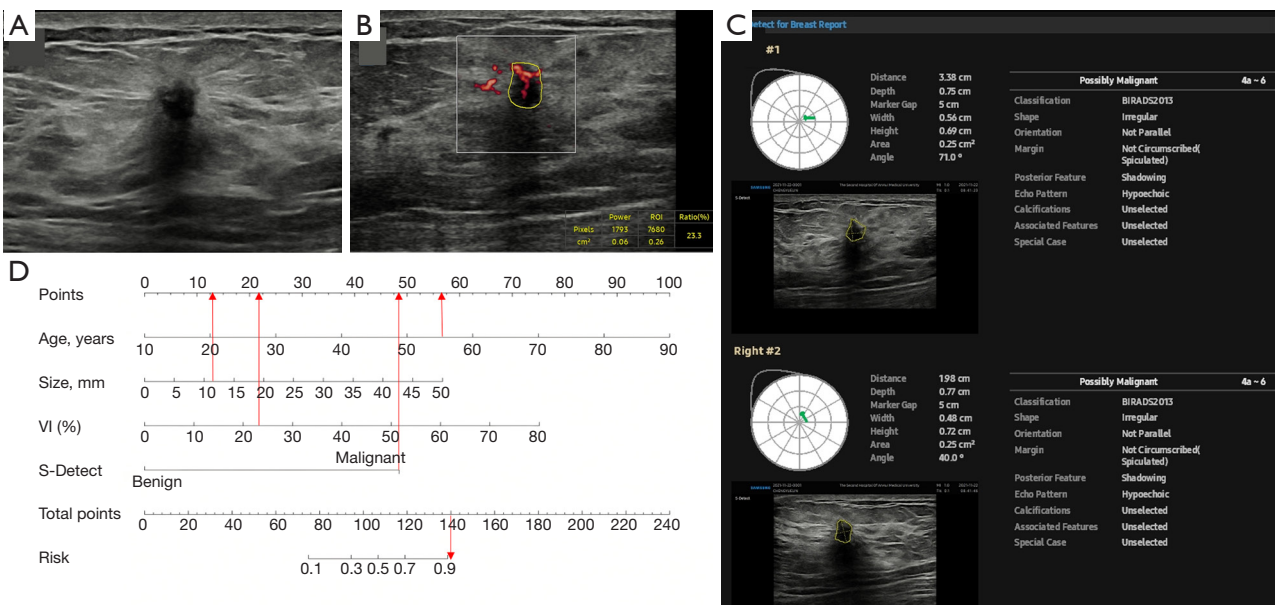

Figure 3 Clinical application of the nomogram. (A) A 56-year-old patient (57 points), with a breast mass 11 mm in diameter (13 points) detected by conventional ultrasound; (B) MVFI showing a VI of 23.3% (22 points); (C) S-Detect-based diagnosis showing malignancy (48 points); and (D) Nomogram showing a total point of 140. Risk of malignancy for breast masses >0.90. Pathological findings: invasive ducal carcinoma. The red arrows indicate the points corresponding to the variable value and the risk corresponding to the total points. The yellow circles indicate the boundary of the mass. MVFI, microvascular flow imaging; VI, vascular index.

clinical and ultrasound image features, variable axes with scales were utilized to demonstrate the interrelationships among the variables. The breast cancer probability for each mass was subsequently determined by summing the points for variable axes. Compared to other prediction models, the nomogram prediction model is more intuitive and facilitates individualized breast cancer risk assessment of patients by clinicians and sonologists. A nomogram can also serve as a practical and easy interdisciplinary communication bridge between clinicians and sonologists. Currently, nomogram models have been used to predict breast disease in many ways, including prediction of breast cancer, breast cancer

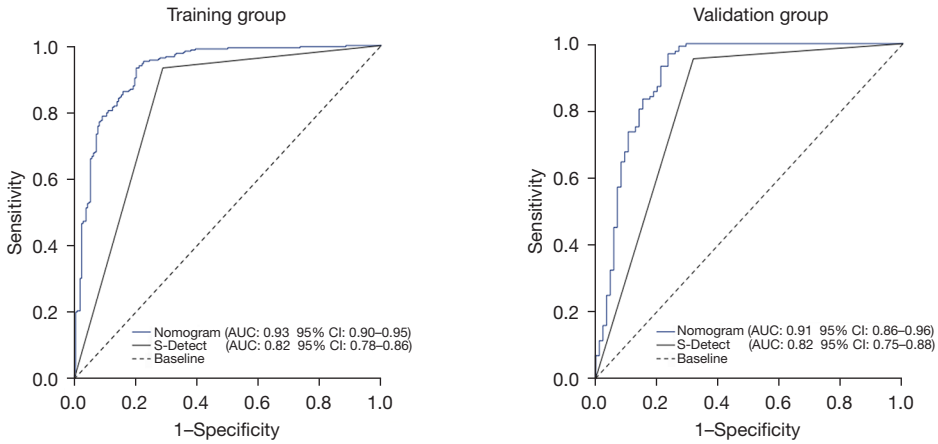

Figure 4 ROC curves for S-Detect and the nomogram model. ROC, receiver operating characteristic; AUC, area under the curve; CI, confidence interval.

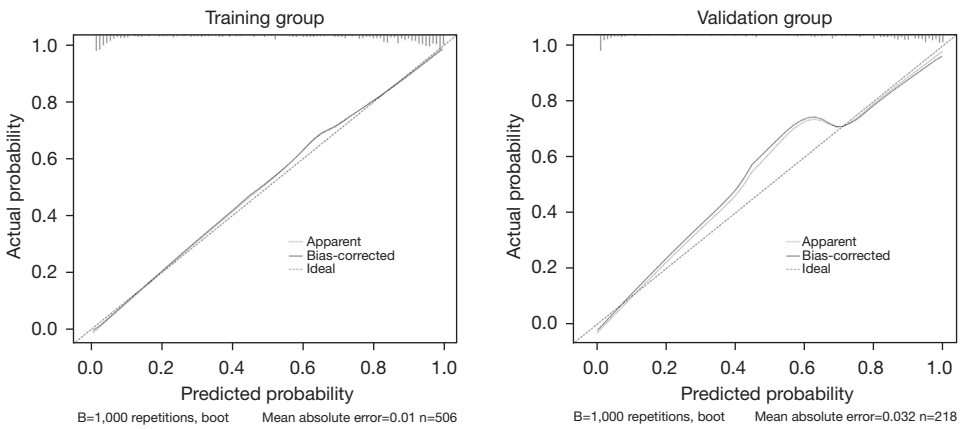

Figure 5 Calibration curves for the nomogram model.

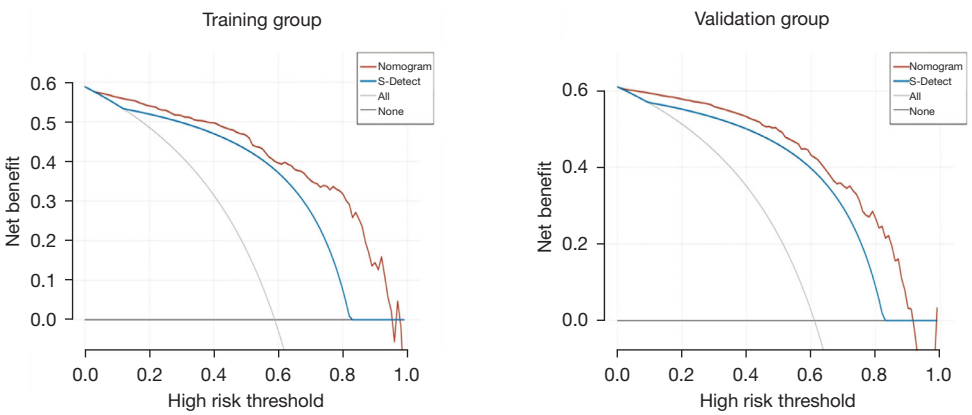

Figure 6 DCA for S-Detect and the nomogram model. DCA, decision curve analysis.

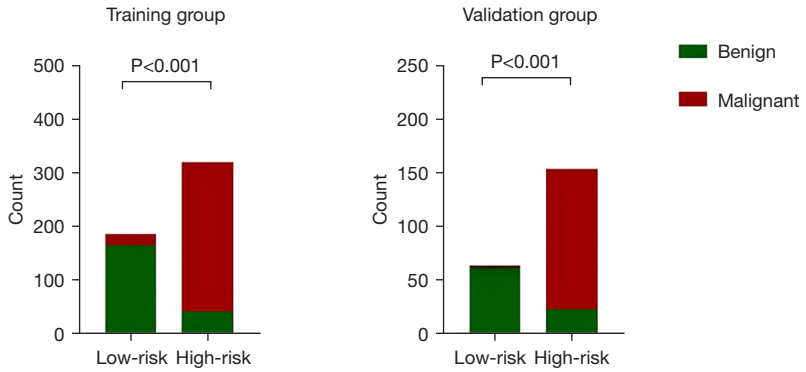

Figure 7 Risk grouping of breast masses.

presenting with axillary lymph node metastasis, breast cancer neoadjuvant chemotherapy to achieve pathologic complete remission response, and breast cancer recurrence and prognosis (22-26). The nomogram model developed in the study was aimed at predicting the risk of masses during breast cancer screening and providing an initial assessment of breast masses.

Wang and Che (27) constructed a nomogram model for predicting breast cancer that incorporated factors such as tumor vascular distribution parameters quantitatively assessed using superb microvascular imaging and BI-RADS classification obtained by conventional ultrasound. The nomogram model constructed by Guo *et al.* (28) was used to assess the risk of breast lesions preoperatively, integrating the results of the Angio Planewave ultrasensitive imaging to determine the blood flow and morphological information of breast lesions obtained through conventional ultrasound. All of these nomogram models showed good predictive performance. In contrast, the nomogram model in the present study was constructed based on quantitative and objective ultrasound and clinical features, all of which are easily accessible and simple to manipulate. The model was expected to objectively evaluate breast masses while minimizing the influence of subjectivity.

S-Detect technology relies on convolutional neural networks and deep learning algorithms. It has become the most widely used AI diagnostic system in breast mass evaluation based on BI-RADS criteria. S-Detect can autonomously recognize and analyze two-dimensional grayscale image features of breast masses, such as shape, orientation, margins, and internal echoes, effectively overcoming subjective bias and providing objective results of benign or malignant evaluations (29). The studies by Zhao *et al.* and Xia *et al.* (30,31) indicated that the diagnostic sensitivity and specificity of S-Detect technology were higher than those of resident sonologists, and its diagnostic capability showed no significant difference compared to that of experienced sonologists. The study by Di Segni *et al.* (32) indicated that the diagnostic sensitivity of S-Detect technology for focal breast lesions exceeded 90% and had a specificity of approximately 70%. These studies have all demonstrated the feasibility of S-Detect technology in predicting breast cancer. Notably, while S-Detect technology has a high sensitivity, its specificity is relatively low. It is likely that this method based on morphological characteristics of breast masses tends to provide a malignant diagnosis to minimize the risk of missing breast cancer. Considering the limitations of using S-Detect technology alone, it was combined with other indicators to enhance the specificity of the diagnosis.

Breast cancer development and progression are highly dependent on angiogenesis. Breast cancer tends to be more richly vascularized than benign breast masses, and these vessels distribute in a twisted, radial pattern around the peripheral and central areas of the mass (33). Therefore, assessment of angiogenesis in breast masses is essential for differentiating malignancy from benignity. MVFI is a novel ultrasound blood flow imaging technology that uses multidimensional filtering to eliminate clutter and motion artifacts, thereby providing a sensitive method for detecting microvessels with low flow velocities, which can be quantitatively assessed by VI (34). This technology has been applied to several organs, including the liver, fetal cranial brain, placenta, thyroid, mammary gland, and cervical lymph nodes, and its value for clinical detection of microvessels has been previously validated (35-39). Bartolotta *et al.* (35) used this technology to detect the vascular distribution of focal breast lesions to distinguish

between benign and malignant lesions, with the final diagnostic AUC, sensitivity, and specificity of 0.70, 76.6%, and 64.1%, respectively. In the present study, the VI quantitatively evaluated the vascular distribution within breast masses as a predictive factor for breast cancer.

Hong *et al.* (40) found that many clinical features are associated with breast cancer, including patient age and mass size, which is in agreement with the present study results. Previous research has confirmed that age is a risk variable influencing the development and prognosis of breast malignancies at the molecular level (41). Breast cancer incidence shows a positive correlation with age, and the risk of malignancy tends to increase with age (42). Chen *et al.* (43) evaluated 1,203 cases of breast masses, and showed that the accuracy of ultrasound diagnosis for masses ≤1 cm, 1.1–2.0 cm, and >2.0 cm in size was 75.6%, 86.4%, and 88.4%, respectively. This is likely because larger breast masses have more typical morphological features, making ultrasound diagnosis easier.

In addition, the cut-off value for the nomogram risk can be utilized for risk stratification. Following risk stratification, special attention should be given to breast masses within the high-risk set, and further evaluation is recommended.

Despite the strengths, this study also has some limitations. First, this single-center study may lead to the potential for bias in our findings; consequently, studies with larger sample sizes and the adoption of a multi-center design are needed in the future to confirm our findings. Second, we only performed the internal validation. Although our predictive model showed great clinical utility, further validation with external groups is needed.

Conclusions

Our constructed nomogram exhibited excellent diagnostic efficacy, calibration, and clinical utility. This nomogram model can quantify the malignancy risk of breast masses, providing a reliable and objective initial assessment to aid in breast cancer screening.

Acknowledgments

None.

Footnote

Reporting Checklist: The authors have completed the TRIPOD reporting checklist. Available at https://gs.amegroups.com/article/view/10.21037/gs-2024-488/rc

Data Sharing Statement: Available at https://gs.amegroups.com/article/view/10.21037/gs-2024-488/dss

Peer Review File: Available at https://gs.amegroups.com/article/view/10.21037/gs-2024-488/prf

Funding: The study was supported by the University Natural Science Research Project of Anhui Province (No. 2023AH040373) and the Clinical Research Cultivation Program of the Second Affiliated Hospital of Anhui Medical University (No. 2021LCZD06).

Conflicts of Interest: All authors have completed the ICMJE uniform disclosure form (available at https://gs.amegroups.com/article/view/10.21037/gs-2024-488/coif). The authors have no conflicts of interest to declare.

Ethical Statement: The authors are accountable for all aspects of the work in ensuring that questions related to the accuracy or integrity of any part of the work are appropriately investigated and resolved. The study received approval from the Medical Research Ethics Committee of the Second Affiliated Hospital of Anhui Medical University (No. SL-YX2022-015) and was conducted in accordance with the Declaration of Helsinki and its subsequent amendments. Individual consent was waived due to the retrospective nature of the analysis.

References

1. Bray F, Laversanne M, Sung H, et al. Global cancer statistics 2022: GLOBOCAN estimates of incidence and mortality worldwide for 36 cancers in 185 countries. CA Cancer J Clin 2024;74:229-63.
2. Wu Q, Xu L. Challenges in HER2-low breast cancer

identification, detection, and treatment. Transl Breast Cancer Res 2024;5:3.
3. Huang J, Chan PS, Lok V, et al. Global incidence and mortality of breast cancer: a trend analysis. Aging (Albany NY) 2021;13:5748-803.
4. Kim J, Kim J, Seo KH, et al. Survival outcomes of young-age female patients with early breast cancer: an international multicenter cohort study. ESMO Open 2024;9:103732.
5. Zhou Y, Li Y, Liu Y, et al. The value of contrast-enhanced energy-spectrum mammography combined with clinical indicators in detecting breast cancer in Breast Imaging Reporting and Data System (BI-RADS) 4 lesions. Quant Imaging Med Surg 2024;14:8272-80.
6. Dan Q, Zheng T, Liu L, et al. Ultrasound for Breast Cancer Screening in Resource-Limited Settings: Current Practice and Future Directions. Cancers (Basel) 2023;15:2112.
7. US Preventive Services Task Force; Nicholson WK, Silverstein M, et al. Screening for Breast Cancer: US Preventive Services Task Force Recommendation Statement. JAMA 2024;331:1918-30.
8. Glechner A, Wagner G, Mitus JW, et al. Mammography in combination with breast ultrasonography versus mammography for breast cancer screening in women at average risk. Cochrane Database Syst Rev 2023;3:CD009632.
9. Shen S, Zhou Y, Xu Y, et al. A multi-centre randomised trial comparing ultrasound vs mammography for screening breast cancer in high-risk Chinese women. Br J Cancer 2015;112:998-1004.
10. Gu Y, Tian J, Ran H, et al. Ultrasound strain elastography to improve diagnostic performance of breast lesions by reclassifying BI-RADS 3 and 4a lesions: a multicentre diagnostic study. Br J Radiol 2025;98:89-99.
11. Jiang X, Chen C, Yao J, et al. A nomogram for diagnosis of BI-RADS 4 breast nodules based on three-dimensional volume ultrasound. BMC Med Imaging 2025;25:48.
12. He X, Lu Y, Li J. Development and validation of a prediction model for the diagnosis of breast cancer based on clinical and ultrasonic features. Gland Surg 2023;12:736-48.
13. Yan M, Peng C, He D, et al. A Nomogram for Enhancing the Diagnostic Effectiveness of Solid Breast BI-RADS 3-5 Masses to Determine Malignancy Based on Imaging Aspects of Conventional Ultrasonography and Contrast-Enhanced Ultrasound. Clin Breast Cancer 2023;23:693-703.
14. Guldogan N, Taskin F, Icten GE, et al. Artificial Intelligence in BI-RADS Categorization of Breast Lesions on Ultrasound: Can We Omit Excessive Follow-ups and Biopsies? Acad Radiol 2024;31:2194-202.
15. Yu ZH, Hong YT, Chou CP. Enhancing Breast Cancer Diagnosis: A Nomogram Model Integrating AI Ultrasound and Clinical Factors. Ultrasound Med Biol 2024;50:1372-80.
16. Wei Q, Yan YJ, Wu GG, et al. The diagnostic performance of ultrasound computer-aided diagnosis system for distinguishing breast masses: a prospective multicenter study. Eur Radiol 2022;32:4046-55.
17. Wang X, Meng S. Diagnostic accuracy of S-Detect to breast cancer on ultrasonography: A meta-analysis (PRISMA). Medicine (Baltimore) 2022;101:e30359.
18. Cai S, Wang H, Zhang X, et al. Superb Microvascular Imaging Technology Can Improve the Diagnostic Efficiency of the BI-RADS System. Front Oncol 2021;11:634752.
19. Dong J, Chen Q, Wang H, et al. A preliminary study on the diagnostic value of contrast-enhanced ultrasound and micro-flow imaging for detecting blood flow signals in breast cancer patients. Gland Surg 2024;13:2098-106.
20. Cai SM, Wang HY, Zhang XY, et al. The Vascular Index of Superb Microvascular Imaging Can Improve the Diagnostic Accuracy for Breast Imaging Reporting and Data System Category 4 Breast Lesions. Cancer Manag Res 2020;12:1819-26.
21. Liang G, Zhang S, Zheng Y, et al. Establishment of a predictive nomogram for breast cancer lympho-vascular invasion based on radiomics obtained from digital breast tomography and clinical imaging features. BMC Med Imaging 2025;25:65.
22. Han Y, Wang J, Sun Y, et al. Prognostic Model and Nomogram for Estimating Survival of Small Breast Cancer: A SEER-based Analysis. Clin Breast Cancer 2021;21:e497-505.
23. Wang SJ, Liu HQ, Yang T, et al. Automated Breast Volume Scanner (ABVS)-Based Radiomic Nomogram: A Potential Tool for Reducing Unnecessary Biopsies of BI-RADS 4 Lesions. Diagnostics (Basel) 2022;12:172.
24. Xu YB, Liu H, Cao QH, et al. Evaluating overall survival and competing risks of survival in patients with early-stage breast cancer using a comprehensive nomogram. Cancer Med 2020;9:4095-106.
25. Hou N, Xiao J, Wang Z, et al. Development and Validation of a Nomogram for Individually Predicting Pathologic Complete Remission After Preoperative Chemotherapy in Chinese Breast Cancer: A Population-Based Study. Clin Breast Cancer 2020;20:e682-94.

26. Wang S, Wang D, Wen X, et al. Construction and validation of a nomogram prediction model for axillary lymph node metastasis of cT1 invasive breast cancer. Eur J Cancer Prev 2024;33:309-20.
27. Wang C, Che Y. A ultrasonic nomogram of quantitative parameters for diagnosing breast cancer. Sci Rep 2023;13:12340.
28. Guo G, Feng J, Jin C, et al. A Novel Nomogram Based on Imaging Biomarkers of Shear Wave Elastography, Angio Planewave Ultrasensitive Imaging, and Conventional Ultrasound for Preoperative Prediction of Malignancy in Patients with Breast Lesions. Diagnostics (Basel) 2023;13:540.
29. Xing B, Fu C, Yang Z. Diagnosis of Benign and Malignant Breast Nodules by Conventional Ultrasound in Combination with S-Detect Technology and Elastic Imaging. J Coll Physicians Surg Pak 2024;34:1154-7.
30. Xia Q, Cheng Y, Hu J, et al. Differential diagnosis of breast cancer assisted by S-Detect artificial intelligence system. Math Biosci Eng 2021;18:3680-9.
31. Zhao C, Xiao M, Jiang Y, et al. Feasibility of computer-assisted diagnosis for breast ultrasound: the results of the diagnostic performance of S-detect from a single center in China. Cancer Manag Res 2019;11:921-30.
32. Di Segni M, de Soccio V, Cantisani V, et al. Automated classification of focal breast lesions according to S-detect: validation and role as a clinical and teaching tool. J Ultrasound 2018;21:105-18.
33. Zhang X, Cheng F, Song X, et al. Superb microvascular imaging for evaluation of microvascularity in breast nodules compared with conventional Doppler imaging. Quant Imaging Med Surg 2023;13:7029-40.
34. Aziz MU, Eisenbrey JR, Deganello A, et al. Microvascular Flow Imaging: A State-of-the-Art Review of Clinical Use and Promise. Radiology 2022;305:250-64.
35. Bartolotta TV, Orlando AAM, Schillaci MI, et al. Ultrasonographic Detection of Vascularity of Focal Breast Lesions: Microvascular Imaging Versus Conventional Color and Power Doppler Imaging. Ultrason Imaging 2021;43:273-81.
36. Leung KY, Wan YL. Update on Color Flow Imaging in Obstetrics. Life (Basel) 2022;12:226.
37. Kang HJ, Lee JM, Jeon SK, et al. Microvascular Flow Imaging of Residual or Recurrent Hepatocellular Carcinoma after Transarterial Chemoembolization: Comparison with Color/Power Doppler Imaging. Korean J Radiol 2019;20:1114-23.
38. Wang T, Xu M, Xu C, et al. Comparison of microvascular flow imaging and contrast-enhanced ultrasound for blood flow analysis of cervical lymph node lesions. Clin Hemorheol Microcirc 2023;85:249-59.
39. Suh PS, Baek JH, Lee JH, et al. Effectiveness of microvascular flow imaging for radiofrequency ablation in recurrent thyroid cancer: comparison with power Doppler imaging. Eur Radiol 2025;35:597-607.
40. Hong ZL, Chen S, Peng XR, et al. Nomograms for prediction of breast cancer in breast imaging reporting and data system (BI-RADS) ultrasound category 4 or 5 lesions: A single-center retrospective study based on radiomics features. Front Oncol 2022;12:894476.
41. Ma X, Liu C, Xu X, et al. Biomarker expression analysis in different age groups revealed age was a risk factor for breast cancer. J Cell Physiol 2020;235:4268-78.
42. Rossi L, Mazzara C, Pagani O. Diagnosis and Treatment of Breast Cancer in Young Women. Curr Treat Options Oncol 2019;20:86.
43. Chen SC, Cheung YC, Su CH, et al. Analysis of sonographic features for the differentiation of benign and malignant breast tumors of different sizes. Ultrasound Obstet Gynecol 2004;23:188-93.

Cite this article as: Hou Z, Zhan Y, Wang J, Peng M. Development and validation of a screening model for benign and malignant breast masses based on S-Detect and microvascular flow imaging. Gland Surg 2025;14(4):687-698. doi: 10.21037/gs-2024-488